THE JOURNAL OF BIOLOGICAL CHEMISTRY VOL. 283, NO. 45, pp. 30950–30956, November 7, 2008

Structural Insights into the Role of Mutations in Amyloidogenesis*[S]

Received for publication, June 24, 2008, and in revised form, August 8, 2008 Published, JBC Papers in Press, September 2, 2008, DOI 10.1074/jbc.M804822200

Elizabeth M. Baden[‡], Edward G. Randles[‡], Awo K. Aboagye[‡], James R. Thompson[§], and Marina Ramirez-Alvarado[‡1]

From the Departments of [‡]Biochemistry and Molecular Biology and [§]Physiology and Biomedical Engineering, College of Medicine, Mayo Clinic, Rochester, Minnesota 55905

Mechanisms of amyloidogenesis are not well understood, including potential structural contributions of mutations in the process. Our previous research indicated that the dimer interface of amyloidogenic immunoglobulin light chain protein AL-09 is twisted 90° relative to the protein from its germline sequence, κI O18/O8. Here we report a systematic restoration of AL-09 to its germline sequence by mutating the non-conservative somatic mutations located in the light chain dimer interface. Among these mutants, we find a correlation between increased thermodynamic stability and an increase in the lag time for fibril formation. The restorative mutant AL-09 H87Y completes the trifecta and restores the dimer interface observed in κI O18/O8, emphasizing the potential importance of the structural integrity of these proteins to protect against amyloidogenicity. We also find that adding amyloidogenic mutations into the germline protein illustrates mutational cooperativity in promoting amyloidogenesis.

Amyloid diseases are characterized by the misfolding of a precursor protein that leads to amyloid fibril formation. Though the precursor proteins are different for each disease, similar mechanisms may cause the amyloidogenesis. In light chain amyloidosis (AL),[2] a monoclonal immunoglobulin light chain (LC) forms amyloid fibrils that deposit in the extracellular space of vital organs (1). Although other precursor proteins may be wild type or linked to a single hereditary mutation, AL is distinct in that hypervariability yields a different set of mutations in each patient. Variable domains of LCs undergo somatic hypermutation, and in the case of AL patients (2), these mutations make proteins thermodynamically destabilized compared with non-amyloidogenic proteins (3–5). Some studies have linked the destabilizing somatic mutations present in AL proteins and the propensity to form amyloid fibrils that leads to cellular and organ damage (4, 6, 7). Studying AL proteins offers a unique opportunity to delineate the role(s) of individual mutations on amyloidogenicity. Comparisons between amyloidogenic and non-amyloidogenic proteins have been made (4, 8), but no systematic study of restorative mutations in a single AL protein has been reported. By restoring the residues found in the corresponding germline sequence, we can assess the contributions of individual residues to amyloidogenicity. Although the mutations in AL proteins are unique to each patient, an underlying structural mechanism may be involved in fibril formation that is common to all pathogenic LC proteins.

When immunoglobulin molecules are secreted, two heavy chains (HCs) usually pair with two LCs to create a heterotetramer. Occasionally, free light chains are secreted (9); these light chains can form homodimers (10). LC dimers can be innocuous, but they can also be pathogenic, as in the case of AL. We previously examined the structure of LC dimer AL-09, a protein isolated from an AL patient (11). AL-09 differs from its germline sequence, κI O18/O8, by seven amino acids. Of these seven somatic mutations, the three non-conservative amino acid changes are located in the dimer interface. We found that the AL-09 dimer has an interface that is rotated 90° from the canonical LC interface observed in the κI O18/O8 protein. The altered interface was accompanied by decreased thermodynamic stability and faster fibril formation for AL-09, compared with κI O18/O8. This was the first time that an altered interface had been observed in an AL protein, fueling our speculation that some of the mutations in AL-09 may be critical to forming the altered interface.

The three non-conservative amino acid changes in the interface that occur between κI O18/O8 and AL-09 are N34I, K42Q, and Y87H (Fig. 1*a*). The interactions in the dimer interface that stabilize the canonical dimer structure may be crucial to preventing amyloidogenicity. Thus, we performed a mutational analysis to test this hypothesis, making restorative mutant proteins with changes at each of these dimer interface positions. The results of this analysis led us to investigate the double restorative mutant (AL-09 I34N/H87Y) as well as a series of reciprocal mutants, in which we start with the κI O18/O8 amino acid sequence and introduce the mutations from the amyloidogenic protein. We then explore the link between thermodynamic stability and fibril formation kinetics and use crystallography to test whether mutants that restore thermodynamic stability also restore the canonical dimer interface to the

* This work was supported, in whole or in part, by National Institutes of Health Grant GM071514 (to M. R.-A.). This work was also supported by Minnesota Partnership for Biotechnology and Medical Genomics Grant SPAP-05-0013-P-FY06 (to J. R. T.) and the Basic Sciences Computing Laboratory of the University of Minnesota Supercomputing Institute (to J. R. T.). The costs of publication of this article were defrayed in part by the payment of page charges. This article must therefore be hereby marked "*advertisement*" in accordance with 18 U.S.C. Section 1734 solely to indicate this fact.

The atomic coordinates and structure factors (codes 3CDY, 3CDF, and 3CDC) have been deposited in the Protein Data Bank, Research Collaboratory for Structural Bioinformatics, Rutgers University, New Brunswick, NJ (http://www.rcsb.org/).

[S] The on-line version of this article (available at http://www.jbc.org) contains Figs. S1 and S2.

[1] To whom correspondence should be addressed: Dept. of Biochemistry and Molecular Biology, College of Medicine, Mayo Clinic, 200 First St. SW, Rochester, MN 55905. Tel.: 507-284-2705; Fax: 507-284-9759; E-mail: ramirezalvarado.marina@mayo.edu.

[2] The abbreviations used are: AL, light chain amyloidosis; LC, light chain; HC, heavy chain; ThT, thioflavin T.

amyloidogenic protein. Our results show that a single amino acid change in the LC dimer interface can restore protein stability, correct the orientation of the dimer interface, and delay amyloid fibril formation.

EXPERIMENTAL PROCEDURES

Site-directed Mutagenesis—The restorative and reciprocal AL-09 mutants were generated by using the QuikChange® Multi Site-directed Mutagenesis kit (Stratagene). The κI O18/O8 germline DNA was generated as described previously (11). The Mayo Clinic DNA Sequencing Core facility confirmed the mutagenesis.

Cloning, Expression, Extraction, and Purification—Recombinant AL-09 and κI O18/O8 proteins were expressed in *Escherichia coli* and purified as described previously (11, 12). AL-09 H87Y, AL-09 Q42K, κI O18/O8 N34I/Y87H, and κI O18/O8 N34I/K42Q/Y87H proteins were expressed and purified by the same method as AL-09. κI O18/O8 Y87H, κI O18/O8 N34I, and AL-09 I34N/H87Y were expressed and purified by the same method as κI O18/O8. AL-09 I34N protein was expressed and purified from both the periplasmic space and inclusion bodies. All proteins were purified by HiLoad 16/60 Superdex 75 column on an AKTA FPLC (GE Healthcare) system. Pure protein was verified by SDS-polyacrylamide gel electrophoresis (SDS-PAGE) and Western blot analysis. The amino acid mutations were verified by Asp-N digestion and mass spectrometry analysis at the Mayo Proteomics Research Center.

Circular Dichroism (CD) Spectroscopy—Protein secondary structure was monitored at 4 °C by far UV-CD (Jasco Spectropolarimeter 810) from 260–200 nm as described in Ref. 11. Thermal denaturation experiments followed the ellipticity at 218 nm over a temperature range of 4–90 °C and were analyzed as described previously (12) to calculate a T_m (melting temperature, where 50% of the protein is unfolded).

Chemical denaturation with urea was carried out by equilibrating 20 μM protein samples overnight at 4 °C in either 0 or 8 M urea. Subsequent samples were generated by exchanging equal volumes of the two stock solutions of 0 and 8 M urea to create a range of urea concentrations while keeping the protein concentration constant. Each sample was equilibrated for 10 min at each urea concentration and then the denaturation experiment was followed by CD, acquiring ellipticity at 218 nm for 60 s or by tryptophan fluorescence, with excitation at 294 nm and an emission scan from 310–400 nm. Alternatively, varying concentrations of urea were added to the protein samples and equilibrated overnight before analyzing as described above. Urea concentration was calculated using a hand refractometer (13). The denaturation curves were analyzed by the same method as described for the thermal denaturation experiment. The C_m is the concentration of denaturant where 50% of the protein is unfolded. $\Delta G_{folding}$ was determined from chemical denaturation data. The enthalpy (ΔH) was determined from the thermal denaturation data using the van't Hoff equation, as described in Ref. 4.

Fibril Formation—Fibril seeds were formed by shaking 750-μl samples of each protein (20 μM protein) in 1.5-ml polypropylene tubes at 300 rpm with 500 mM Na_2SO_4 and 0.02% NaN_3 in 10 mM Tris-HCl (pH 7.4) buffer. Temperature for fibril formation was the melting temperature in the presence of 500 mM Na_2SO_4 (T_{mNaS}) of each protein (Table 1). ThT fluorescence was monitored to follow fibril formation. A 3-μl fibril sample was added to 5 μM ThT, and the fluorescence emission was measured (PTI-QM2001 fluorometer). The excitation wavelength was 450 nm, and the emission was scanned from 470–530 nm. The concentration of seeds was determined by pelleting the fibrils and measuring the concentration of the soluble protein. This concentration was subtracted from the initial protein concentration to find the fibril concentration. Before they were used to seed further reactions, the fibrils were washed three times with buffer to remove Na_2SO_4.

Fibril formation kinetics were followed (with each protein in triplicate in a 96-well plate) by measuring ThT fluorescence on a plate reader (Analyst AD, Molecular Devices) with an excitation wavelength of 430 nm and an emission wavelength of 485 nm. Plates were incubated at 37 °C in a temperature-controlled incubator and shaken continuously on a Lab-Line titer plate shaker (speed setting 3). Each well contained 20 μM protein, a 1:20 ratio of seeds to soluble protein, 150 mM NaCl, 0.02% NaN_3, and 5 μM ThT in 10 mM Tris-HCl buffer (pH 7.4). Total volume for each reaction was 260 μl.

Electron Microscopy (EM)—A 3-μl fibril sample was placed on a 300 mesh copper formvar/carbon grid and air-dried. The sample was negatively stained with 4% uranyl acetate, washed, air-dried, and inspected on a Philips Technai T12 transmission electron microscope.

Crystallization/X-ray Data Collection—Purified κI O18/O8 Y87H, κI O18/O8 N34I/Y87H, and AL-09 H87Y proteins were concentrated to 1.04 mM, 1.17 mM, and 900 μM, respectively, in 10 mM Tris-HCl buffer (pH 7.4). AL-09 H87Y crystals were obtained in hanging drops using vapor diffusion against 30% w/v polyethylene glycol 4000 and 0.2 M Li_2SO_4 in 0.1 M Tris buffer (pH 8.3) at 22 °C. A 2-μl aliquot of the protein solution was mixed with an equal volume from each reservoir. The equilibrated conditions were suitable for cryoprotection of crystals by flash-cooling in liquid N_2. κI O18/O8 Y87H crystals were obtained in a similar manner, using vapor diffusion against 1.2 M sodium citrate in 0.1 M Tris buffer pH 8.1. κI O18/O8 N34I/Y87H crystals were obtained using vapor diffusion against 1.1 M sodium citrate in 0.1 M Tris buffer pH 8.3. κI O18/O8 N34I/K42Q/Y87H crystals were obtained using vapor diffusion against 1.3 M sodium citrate in 0.1 M Tris buffer pH 8.1, with a thin layer of 40% paraffin oil and 60% silicon oil. The latter three crystals were briefly soaked in 15% glycerol to be suitable for cryoprotection. AL-09 H87Y data were collected at wavelength 0.979508 nm on beamline 19BM at Argonne National Laboratory. Data for the other three proteins were collected at 1.5241 nm. All data were collected at 100 K. Table 3 summarizes the statistics for the crystallographic diffraction data collections and structural refinement.

Structure Refinement—Diffraction data for AL-09 H87Y were processed with HKL2000 and SCALEPACK (14). Diffraction data for κI O18/O8 Y87H, κI O18/O8 N34I/Y87H, and κI O18/O8 N34I/K42Q/Y87H were processed with Crystal Clear (15). All structures were solved by molecular replacement with the κI O18/O8 structure (Protein Data Bank code 2Q20) using PHASER (16, 17). Programs REFMAC5 (18) and COOT (19)

TABLE 1
Thermodynamics of restorative and reciprocal mutants

Protein[a]	T_m	T_{mNaS}	C_m	$\Delta G_{folding}$	ΔH
	°C	°C	M	kcal/mol	kcal/mol
AL-09[b]	41.1 ± 1.0[c]	50.4 ± 0.6	1.88 ± 0.07	-3.53 ± 0.28	-62.8 ± 1.0
κI O18/O8 N34I/Y87H	39.5 ± 1.0	50.8 ± 0.3	1.89 ± 0.06	-3.81 ± 0.66	-79.7 ± 4.24
AL-09 Q42K	40.2 ± 0.3	50.4 ± 0.3	1.80 ± 0.25	-4.20 ± 0.86	-75.3 ± 1.8
κI O18/O8 Y87H	47.3 ± 0.4	59.6 ± 0.7	2.98 ± 0.28	-4.58 ± 0.38	-77.3 ± 3.5
κI O18/O8 N34I/K42Q/Y87H	39.4 ± 0.3	50.3 ± 1.2	1.83 ± 0.18	-4.74 ± 0.61	-86.2 ± 5.5
AL-09 I34N	48.6 ± 0.2	58.8 ± 0.3	2.92 ± 0.22	-5.34 ± 0.72	-77.3 ± 2.4
AL-09 H87Y	54.6 ± 0.6	64.3 ± 0.5	3.29 ± 0.04	-6.10 ± 0.30	-100.1 ± 10.3
κI O18/O8[c]	56.1 ± 0.2	68.0 ± 0.3	3.98 ± 0.07	-6.12 ± 0.23	-95.7 ± 2.6
AL-09 I34N/H87Y	58.0 ± 0.1	69.6 ± 0.2	4.52 ± 0.16	-6.84 ± 1.27	-100.5 ± 7.4
κI O18/O8 N34I	51.5 ± 0.9	65.3 ± 0.3	3.06 ± 0.17	-7.17 ± 1.50	-109.5 ± 8.5

[a] Proteins are in order from least to most favorable $\Delta G_{folding}$.
[b] Data previously reported in Ref. 11.
[c] Error is the S.D. of at least three independent experiments.

were used for structure refinement and model building. TLS (translational/libration/screw-rotational) parameters were used to model atomic displacements (20) with one TLS domain set for each monomer within the asymmetric unit. The stereochemistry and the agreement between model and x-ray data were verified by COOT, MOLPROBITY (21), PROCHECK (22), and SFCHECK (23). The Ramachandran outliers for AL-09 H87Y, κI O18/O8 Y87H, and κI O18/O8 N34I/Y87H were 0.00%. AL-09 H87Y had 95.28% in favored Ramachandran orientations, κI O18/O8 Y87H had 95.15% and κI O18/O8 N34I/Y87H had 94.39%. Coordinates for the final structures reported have been deposited into the Protein Data Bank with codes 3CDY, 3CDF, and 3CDC for AL-09 H87Y, κI O18/O8 Y87H, and κI O18/O8 N34I/Y87H, respectively.

RESULTS

Thermodynamic Stability of Mutants—All of the restorative and reciprocal mutants exhibit the expected β-sheet secondary structure as measured by far-UV circular dichroism (CD) (data not shown). The thermodynamics of the mutants, as followed by thermal and chemical denaturation experiments, are compared in Table 1. For the AL-09 restorative mutants, in which individual dimer interface residues are restored to those found in κI O18/O8, the most striking result comes from restoring the histidine to tyrosine at position 87 (H87Y). With this single mutation, AL-09 H87Y regains most of the thermodynamic stability found in κI O18/O8 (Fig. 1*b*), with T_m values (temperature at which 50% of the protein is folded) of 54.6 and 56.1 °C, respectively. This is nearly 15 °C higher than the T_m for amyloidogenic AL-09. In addition, the non-conservative interface mutation AL-09 I34N restores half of the stability to AL-09. The AL-09 Q42K mutation, however, remains as unstable as the amyloidogenic protein (Fig. 1*b*). Exploring the combined effects of the stabilizing mutations, the double restorative mutant AL-09 I34N/H87Y increases the thermodynamic stability even slightly beyond that of κI O18/O8. The C_m (concentration of urea where 50% of the protein is folded), $\Delta G_{folding}$ and ΔH values also follow similar trends (Table 1).

After observing the huge change in stability with AL-09 H87Y, we decided to create reciprocal mutants as well. In this case, we change key interface residues in κI O18/O8 to the corresponding amino acids in AL-09 to determine if a particular mutation or combination of mutations is significantly destabilizing. Both κI O18/O8 N34I and κI O18/O8 Y87H decrease the stability, by 4.6 and 8.8 °C, respectively (Table 1 and Fig. 1*c*). Although the effects of the single reciprocal mutations are not quite as dramatic as restoring AL-09 H87Y, the combined effect of these two mutations in κI O18/O8 N34I/Y87H drastically diminishes the stability, making it comparable to AL-09. Mutating all of the residues that change in the dimer interface creates a similarly destabilized protein in κI O18/O8 N34I/K42Q/Y87H. Together, the restorative and reciprocal mutants indicate a key role for the dimer interface residues at positions 34 and 87.

Amyloid Fibril Formation Kinetics Follow Thermodynamic Stability Trend—A previous study from our laboratory indicated that the kinetics of fibril formation differ between κI O18/O8 and AL-09 in correlation with their differences in thermodynamic stability. AL-09 fibril formation occurs in just 24 h, compared with κI O18/O8, where fibril formation is delayed until 216 h (11). We followed fibril formation reactions to determine whether the restorative and reciprocal mutants also have a similar correlation between thermodynamic stability and fibril formation kinetics.

Table 2 summarizes the results of the fibril formation reactions, which were assessed by ThT fluorescence (supplemental Fig. S1) and electron microscopy (Fig. 2). Our criteria for fibril formation included the time point at which the ThT fluorescence enhancement indicated a plateau in fibril formation and where electron microscopy confirmed fibril formation.

κI O18/O8 N34I/Y87H, which is destabilized as much as AL-09, follows a similar fibril formation pattern to the amyloidogenic protein, forming fibrils within 24 h. κI O18/O8 N34I/K42Q/Y87H also forms fibrils within 24 h and has a similar thermodynamic profile compared with both AL-09 and κI O18/O8 N34I/Y87H. AL-09 I34N and κI O18/O8 Y87H, which have intermediate levels of stability, form fibrils more slowly than AL-09, but more quickly than κI O18/O8. As expected from its increased thermodynamic stability, AL-09 H87Y significantly delays fibril formation (264 h) compared with amyloidogenic AL-09.

The double restorative mutant, AL-09 I34N/H87Y, surpasses the amount of time needed for κI O18/O8 to form fibrils by over 100 h (Table 2). The increase in time for fibril formation corresponds to an increase in $\Delta G_{folding}$ values between −6.12 and

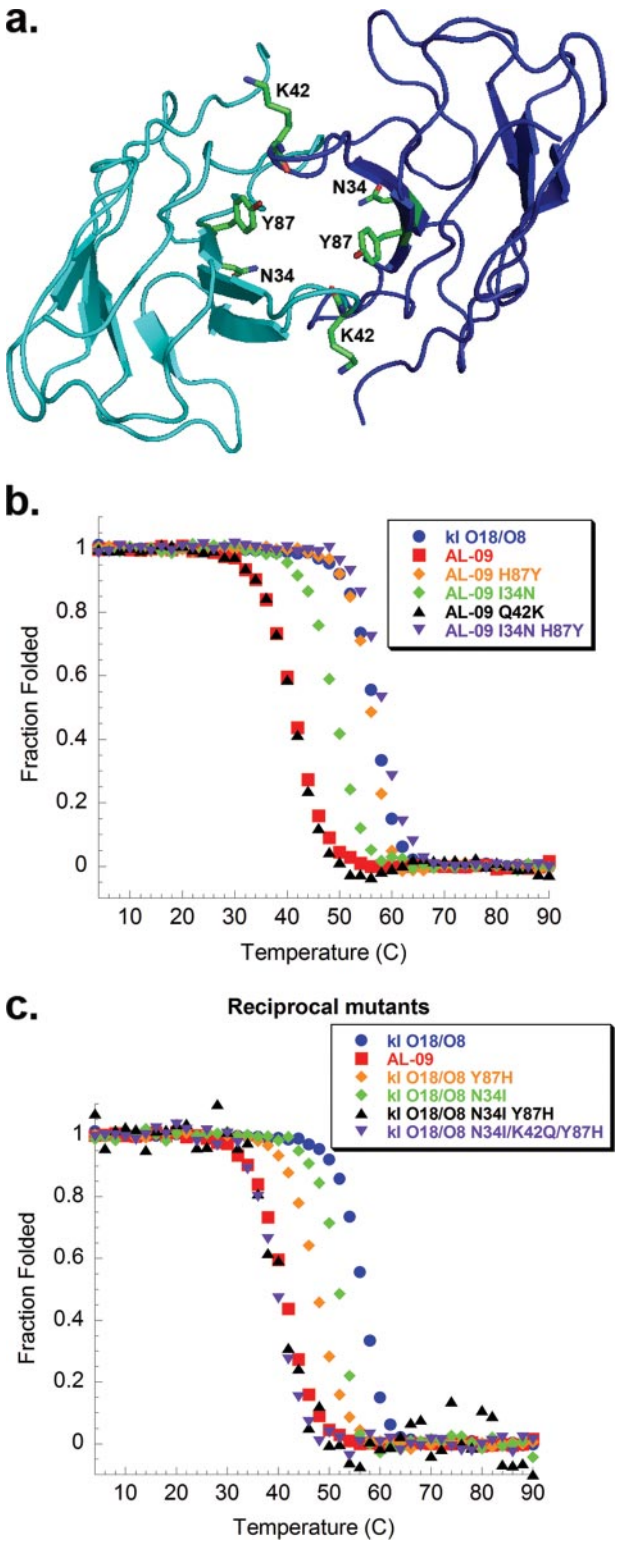

FIGURE 1. **Interface mutations and thermodynamic stability comparison of restorative and reciprocal mutants.** *a*, κI O18/O8 dimer structure with monomers in *blue* and *cyan*. Positions of mutations in the dimer interface of AL-09 are shown in *green*. *b*, thermal denaturation studies of the restorative mutants indicate that AL-09 H87Y, AL-09 I34N, and the double restorative mutant all increase in thermodynamic stability compared with AL-09. *c*, thermal denaturation of the single reciprocal mutants shows some destabilizing effects, and the double reciprocal mutant is completely destabilized to the same extent as amyloidogenic AL-09.

TABLE 2
Fibril formation (seeded) at 37 °C

Protein[a]	Fibril formation (hours)[b]
AL-09	24
κI O18/O8 N34I/Y87H	24
AL-09 Q42K	336
κI O18/O8 Y87H	96
κI O18/O8 N34I/K42Q/Y87H	24
AL-09 I34N	72
AL-09 H87Y	264
κI O18/O8	216
AL-09 I34N/H87Y	360
κI O18/O8 N34I	500

[a] Proteins are in order from least to most favorable $\Delta G_{folding}$.
[b] The number of hours reported is taken from the average of at least three experiments.

−6.84 kcal/mol for κI O18/O8 and AL-09 I34N/H87Y, respectively.

κI O18/O8 N34I requires 500 h to form amyloid fibrils, the longest of any of the proteins studied. While the T_m of this protein places its stability between AL-09 and κI O18/O8, κI O18/O8 N34I actually has the highest $\Delta G_{folding}$ of any of the proteins. Thus, the lengthy lag time for fibril formation correlates with this thermodynamic parameter.

AL-09 Q42K is the lone protein that does not appear to follow the trend linking thermodynamic stability with the kinetics of amyloid fibril formation. Although it is destabilized as much as AL-09, it did not form fibrils until 336 h. It is possible that the amino acid change involved with this restorative mutation sufficiently alters the interactions between the protein and its environment to affect the amyloid formation pathway and delay fibril formation more than expected.

Restorative Mutant Restores Dimer Interface—Because the AL-09 H87Y mutant restores most of the thermodynamic stability and delays fibril formation even longer than κI O18/O8, we wanted to determine if restoring that single mutation affects the protein structure, especially with respect to the dimer interface. Similarly, we wanted to determine if introducing amyloidogenic mutations to κI O18/O8 Y87H and κI O18/O8 N34I/Y87H alters the dimer interfaces of those proteins.

Solving the crystal structure of AL-09 H87Y to 2.43 Å resolution reveals that the lone amino acid change in the amyloidogenic protein is enough to restore the canonical dimer interface found in κI O18/O8 (Fig. 3*a* and Table 3). Superposition of AL-09 H87Y with κI O18/O8 does not show any significant differences between the two structures, and the hydrogen bonding and other nonbonding interactions are nearly identical. In an attempt to learn more about the dynamic nature of the dimer interface, ^{15}N ^{1}H HSQC spectra were acquired for κI O18/O8 and AL-09 at 500 μM protein concentration (data not shown). Although these spectra show many chemical shift differences between the proteins, peak broadening prevented full assignment of the residues in the dimer interface. In contrast, little or no broadening was observed in HSQC spectra of AL-09 H87Y, the only protein with a predominantly dimeric population at this concentration (K_d = 200 nm, compared with κI O18/O8, where K_d = 217 μM and AL-09, where K_d = 23 μM) (11).

Our striking results with AL-09 H87Y led us to assess the number of amyloidogenic mutations required to create the altered dimer interface observed for AL-09 by determining

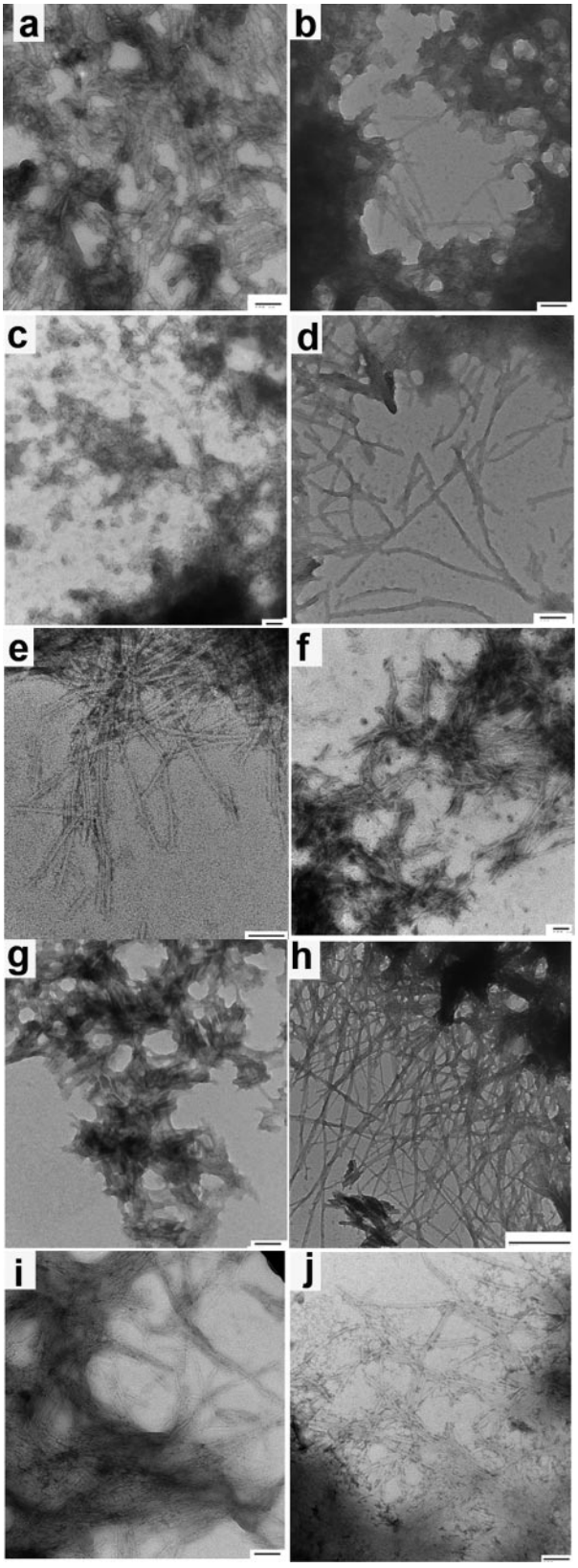

FIGURE 2. **Electron microscopy confirms the formation of amyloid fibrils.** *a*, AL-09 after 44 h; *b*, κI O18/O8 N34I/Y87H after 24 h; *c*, AL-09 Q42K after 336 h; *d*, κI O18/O8 Y87H after 96 h; *e*, κI O18/O8 N34I/K42Q/Y87H after 24 h; *f*, AL-09 I34N after 72 h; *g*, AL-09 H87Y after 264 h; *h*, κI O18/O8 after 288 h; *i*, AL-09 I34N/H87Y after 360 h; *j*, κI O18/O8 N34I after 500 h. Proteins are shown in the order of increasing stability as measured by $\Delta G_{folding}$, corresponding to Table 2. Scale bar for κI O18/O8 is 500 nm; all others are 100 nm.

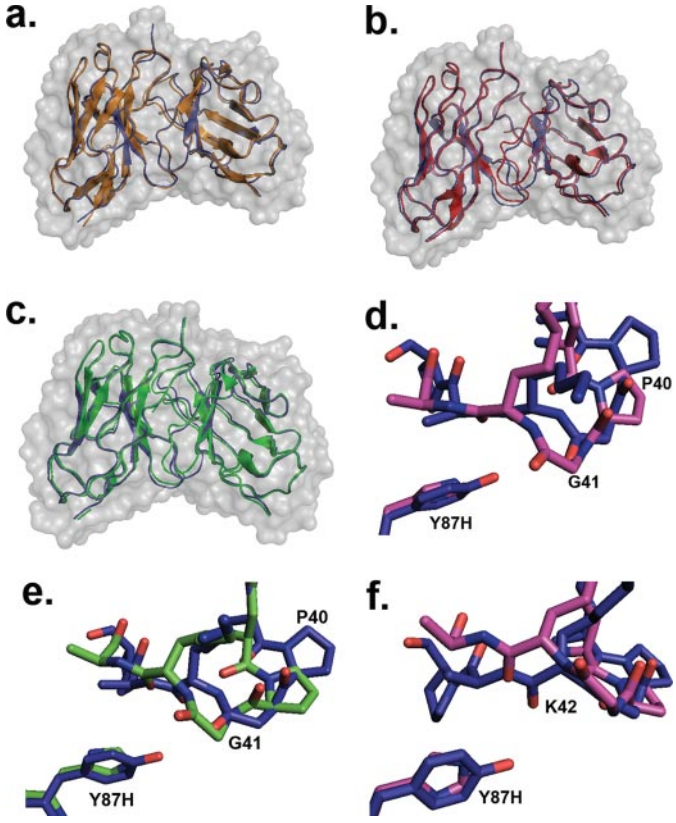

FIGURE 3. **Crystal structures show canonical dimer interface and destabilized loops.** *a*, superposition of κI O18/O8 (*blue*) and AL-09 H87Y (*orange*) shows restored dimer interface. *b*, differences in the loop between Lys-39 and Pro-44 are visible in the global superposition of κI O18/O8 (*blue*) and κI O18/O8 Y87H (*red*). *c*, superposition of κI O18/O8 (*blue*) and κI O18/O8 N34I/Y87H (*green*) shows a change in the same loop as observed in *b*. *d*, shift of Pro-40 and Gly-41 in the κI O18/O8 Y87H mutant (*pink*) disrupts an interaction between Tyr-87 and the carbonyl of Gly-41. *e*, detailed view of Pro-40 and Gly-41 of κI O18/O8 (*blue*) and κI O18/O8 N34I/Y87H (*green*) shows same disrupted interaction as observed with the κI O18/O8 Y87H mutant in *d*. *f*, hydrogen bonding between the backbone carbonyl of Lys-42 and the OH of Tyr-87 in κI O18/O8 (*blue*) is lacking with the His-87 mutation in κI O18/O8 Y87H (*pink*). This is also observed in the κI O18/O8 N34I/Y87H mutant (not pictured).

the crystal structures of three reciprocal mutants. The κI O18/O8 Y87H reciprocal mutation was not enough to singlehandedly alter the dimer interface (Fig. 3*b*). However, we did find evidence of disruption caused by this mutation. In the structure, solved to 1.56-Å resolution, the 40–44 loop (containing residues ^{40}PGKAP^{44}) shows that the backbone is shifted in the κI O18/O8 Y87H mutant. Specifically, the Cα of Pro-40 is shifted by 2.92 Å, and the Cα of Gly-41 is shifted by 3.08 Å compared with κI O18/O8 (Fig. 3*d*). Also, in κI O18/O8, a hydrogen bond between the backbone carbonyl of Lys-42 on chain A and Tyr-87 on the opposite subunit effectively pulls the loop around into the dimer interface (Fig. 3*f*). With κI O18/O8 Y87H, however, the loss of the tyrosine prevents this interaction and the loop shifts back away from the interface. In addition to these measurable shifts, the mutation to His-87 likely alters interactions that involve hydrogen bonding through water in the region surrounding that residue.

Although κI O18/O8 N34I/Y87H differs significantly from κI O18/O8 Y87H with regard to thermodynamic stability and fibril formation properties, not many differences were found

TABLE 3
Data collection and refinement statistics (molecular replacement)

	AL-09 H87Y	κI O18/O8 Y87H	κI O18/O8 N34I/Y87H
Data collection[a]			
Space group	$P6_1$	$P2_1$	$P6_1$
Cell dimensions			
a, *b*, *c* (Å)	74.0, 74.0, 95.1	73.0, 98.0, 73.0	73.8, 73.8, 97.5
a, b, g (°)	90, 90, 120	90, 119.60, 90	90, 90, 120
Resolution (Å)	50-2.43 (2.52-2.43)[b]	17.56-1.39 (1.44-1.39)	34.52-1.33 (1.38-1.33)
R_{sym} or R_{merge}	0.101 (0.365)	0.043 (0.325)	0.052 (0.483)
$I/\sigma I$	39.4 (7.9)	14.5 (1.9)	12.0 (1.4)
Completeness (%)	94.1 (91.5)	73.7 (13.9)	93.8 (45.1)
Redundancy	11.2 (10.4)	3.31 (1.82)	6.38 (1.71)
Refinement			
Resolution (Å)	64.02-2.43 (2.49-2.43)	17.56-1.56 (1.60-1.56)	34.52-1.53 (1.57-1.53)
No. reflections	9593 (706)	109155 (8204)	43135 (3189)
R_{work}/R_{free}	18.9/26.3	17.3/21.8	18.9/23.1
Completeness (%)		86.5 (88.7)	99.9 (99.8)
No. atoms			
Protein	1696	5536	1806
Water	89	1056	403
***B*-factors**			
Protein	50.411	11.975	21.557
Water	45.837	27.447	39.297
r.m.s.[c] deviations			
Bond lengths (Å)	0.019	0.016	0.019
Bond angles (°)	1.789	1.541	1.857

[a] One crystal was used to determine each structure.
[b] Values in parentheses are for highest-resolution shell.
[c] r.m.s., root mean square.

between the two crystal structures. κI O18/O8 N34I/Y87H, solved to 1.53-Å resolution, maintains the canonical dimer interface (Fig. 3*c*). However, we did observe an effect on the 40–44 loop that was similar to the κI O18/O8 Y87H mutant (Fig. 3*e*). In this case, the Cα shifts compared with κI O18/O8 are 2.27 Å for Pro-40 and 2.04 Å for Gly-41. κI O18/O8 N34I/Y87H also lacks the hydrogen bond between Lys-42 on chain A and residue 87 on chain B (electron density, supplemental Fig. S2); the distance between these residues is even greater than that observed in the κI O18/O8 Y87H mutant (4.95 Å compared with 3.54 Å). Although the addition of the N34I mutation may be expected to cooperate to alter the dimer interface based on its loss of thermodynamic stability, it is possible that when all of the mutations are present in AL-09, Ile-34 is destabilizing. In the context of the double mutant, however, it could have a compensatory effect stabilizing the structure.

To completely assess the role of the non-conservative mutations in the dimer interface, we also solved the structure of the triple reciprocal mutant κI O18/O8 N34I/K42Q/Y87H to 3.0-Å resolution (data not shown). This protein also retained the canonical dimer interface, indicating that introducing the interface mutations from the amyloidogenic protein is not alone sufficient to populate the alternate dimer conformation observed for AL-09 by x-ray crystallography.

DISCUSSION

Our analysis highlights a single AL-09 mutation, His-87, which, when restored to the tyrosine residue found in κI O18/O8, regains thermodynamic stability, delays amyloid formation, and restores the canonical dimer interface. The restorative and reciprocal mutations in the amyloidogenic protein AL-09 show a correlation between protein stability and the kinetics of amyloid fibril formation, as well as a link between the mutations and protein stability. Fibril formation studies establish that less stable forms of the protein AL-09 form fibrils faster than more stable mutants.

This study is not the first time that the His-87 mutation has been shown to have a critical role in an LC protein. MOPC 21 is a κIV murine myeloma protein that cannot be secreted unless complexed with HC. Dul *et al.* (24) study the mechanism of the secretory defect and find that it is caused by the single amino acid mutation, His-87. Upon restoring the germline tyrosine residue, the protein regains a normal secretory phenotype, much as restoring H87Y to AL-09 restored a germline-like phenotype to that protein. The importance of this mutation is also reinforced by the finding that Tyr-87 is >95% conserved across all κ and λ germline sequences (11).

The fibril formation kinetics assays with the AL-09 and κI O18/O8 mutants not only illustrate a link between protein stability and capacity for amyloid formation, but they also show that a single mutation in the κI O18/O8 germline protein can greatly increase its amyloidogenic propensity. The κI O18/O8 Y87H mutant, for example, formed fibrils within 96 h, about twice as fast as κI O18/O8. Introducing two mutations, κI O18/O8 N34I/Y87H, accelerated fibril formation even further, to 24 h, which is on par with amyloidogenic AL-09. Previous studies with non-amyloidogenic LC protein LEN found a similar pattern, in which introducing just one or two mutations from AL protein SMA caused LEN to become fibrillogenic (25).

Other studies linking specific amino acids to amyloidogenicity also correlate with our results that less stable proteins form fibrils more quickly. Hurle *et al.* (6) studied several AL κ LC sequences and found rare mutations that occur at structurally important positions. They then introduced these single-point

mutations into non-amyloidogenic Bence Jones protein REI and found that the less stable proteins aggregated more than proteins with higher stability.

Del Pozo Yauner *et al.* (26) compare a λ6a germline protein to a λ6a R25G mutant. Their findings are similar to our results in that the λ6a germline is more stable than λ6a R25G and also delays fibrillogenesis. The authors postulate that the R25G mutation may destabilize the N-terminal loop, causing increased fibril formation.

A study by Wall *et al.* (8) also illustrates the importance of certain structural elements in conjunction with fibrillogenesis. This study introduced two neutral mutations to disrupt an electrostatic interaction in a relatively stable multiple myeloma LC protein (Jto). These neutral mutations simulate the context of another, highly fibrillogenic protein (Wil). The authors found that one of the mutants was comparable to Jto in thermodynamics and fibril formation kinetics, but a second mutant had several side chain alterations that led to a different hydrophobic surface and electrostatic interactions. This second mutant had an increased rate of fibrillogenesis. Among the proteins that we studied, we also observed mutations altering electrostatic and hydrogen bonding interactions that ultimately led to the shifted loop regions in κI O18/O8 Y87H and κI O18/O8 N34I/Y87H. These shifts were accompanied by increases in the propensity for amyloid formation and decreased thermodynamic stability.

Our structural analysis of the reciprocal mutants, in which we changed amino acids from the germline sequence to their amyloidogenic counterparts, did not reveal an altered dimer interface for either the critical κI O18/O8 Y87H mutation or the thermodynamically unstable κI O18/O8 N34I/Y87H or κI O18/O8 N34I/K42Q/Y87H proteins. Similarly, when Dul *et al.* (24) introduced the His-87 mutation from the pathogenic protein into a wild-type λ germline, secretion was not inhibited.

The reciprocal mutants also reveal destabilization of the 40–44 loop. This region is also shifted in κI AL protein BRE when compared with a non-amyloidogenic protein (27). Crystallization studies of other AL proteins, AL-12 and AL-103, have also shown the 40–44 loop to be disordered.[3] Therefore, this region may be a key to amyloidogenic propensity in LC proteins.

Though none of the reciprocal mutants displayed a drastic change like the altered and restored dimer interfaces in AL-09 and AL-09 H87Y, similar subtle structural changes have been shown to be important in another amyloid disease precursor protein as well. In transthyretin (TTR) amyloidosis, the EF-helix becomes slightly more disordered as the pH decreases, and this may be the mechanism by which mutations in this region are more amyloidogenic (28). Thus, seemingly small changes in the structure of amyloid precursor proteins may have a huge impact on amyloidogenicity.

Collectively, our results lead us to conclude that for AL proteins, a single mutation is unlikely to cause a protein to become amyloidogenic. Rather, it is plausible that the combinatorial interactions of destabilizing and compensatory mutations lead to pathogenesis, and minor disruptions in the structure could significantly increase the protein amyloidogenic propensity. The altered interface observed in AL-09 may be evidence that this protein populates a dimer that is less prevalent in κI O18/O8 and the mutants that we studied.

[3] E. G. Randles, D. J. Martin, J. R. Thompson, and M. Ramirez-Alvarado, submitted for publication.

Acknowledgments—We thank Brian Volkman and Francis Peterson for assistance with NMR analysis and helpful discussions. We acknowledge use of Argonne National Laboratory's APS for collection of the x-ray diffraction data for AL-09 H87Y.

REFERENCES

1. Kyle, R. A., and Gertz, M. A. (1995) *Semin. Hematol.* **32,** 45–59
2. Comenzo, R. L., Wally, J., Kica, G., Murray, J., Ericsson, T., Skinner, M., and Zhang, Y. (1999) *Br. J. Haematol.* **106,** 744–751
3. Stevens, P. W., Raffen, R., Hanson, D. K., Deng, Y. L., Berrios-Hammond, M., Westholm, F. A., Murphy, C., Eulitz, M., Wetzel, R., Solomon, A., Schiffer, M., and Stevens, F. J. (1995) *Protein Sci.* **4,** 421–432
4. Wall, J., Schell, M., Murphy, C., Hrncic, R., Stevens, F. J., and Solomon, A. (1999) *Biochemistry* **38,** 14101–14108
5. Kim, Y., Wall, J. S., Meyer, J., Murphy, C., Randolph, T. W., Manning, M. C., Solomon, A., and Carpenter, J. F. (2000) *J. Biol. Chem.* **275,** 1570–1574
6. Hurle, M. R., Helms, L. R., Li, L., Chan, W., and Wetzel, R. (1994) *Proc. Natl. Acad. Sci. U. S. A.* **91,** 5446–5450
7. Wetzel, R. (1997) *Adv. Protein Chem.* **50,** 183–242
8. 8 Wall, J. S., Gupta, V., Wilkerson, M., Schell, M., Loris, R., Adams, P., Solomon, A., Stevens, F., and Dealwis, C. (2004) *J. Mol. Recognit.* **17,** 323–331
9. Dul, J. L., and Argon, Y. (1990) *Proc. Natl. Acad. Sci. U. S. A.* **87,** 8135–8139
10. Stevens, F. J., Westholm, F. A., Solomon, A., and Schiffer, M. (1980) *Proc. Natl. Acad. Sci. U. S. A.* **77,** 1144–1148
11. Baden, E. M., Owen, B. A., Peterson, F. C., Volkman, B. F., Ramirez-Alvarado, M., and Thompson, J. R. (2008) *J. Biol. Chem.* **283,** 15853–15860
12. McLaughlin, R. W., De Stigter, J. K., Sikkink, L. A., Baden, E. M., and Ramirez-Alvarado, M. (2006) *Protein Sci.* **7,** 1710–1722
13. Pace, C. N., and Scholtz, M. (1997) in *Protein Structure, A Practical Approach* (Creighton, T. E., ed) pp. 299–321, Oxford University Press, New York
14. Otwinowski, Z., and Minor, W. (1997) *Methods Enzymol.* **276,** 307–326
15. Pflugrath, J. W. (1999) *Acta Crystallogr. D. Biol. Crystallogr.* **55,** 1718–1725
16. Storoni, L. C., McCoy, A. J., and Read, R. J. (2004) *Acta Crystallogr. D. Biol. Crystallogr.* **60,** 432–438
17. Read, R. J. (2001) *Acta Crystallogr. D. Biol. Crystallogr.* **57,** 1373–1382
18. Murshudov, G. N., Vagin, A. A., and Dodson, E. J. (1997) *Acta Crystallogr. D. Biol. Crystallogr.* **53,** 240–255
19. Emsley, P., and Cowtan, K. (2004) *Acta Crystallogr. D Biol. Crystallogr.* **60,** 2126–2132
20. Winn, M. D., Isupov, M. N., and Murshudov, G. N. (2001) *Acta Crystallogr. D Biol. Crystallogr.* **57,** 122–133
21. Richardson, J. S., Bryan, W. A., 3rd, and Richardson, D. C. (2003) *Methods Enzymol.* **374,** 385–412
22. Laskowski, R. A., MacArthur, M. W., Moss, D. S., and Thornton, J. M. (1993) *J. Appl. Crystallogr.* **26,** 283–291
23. Vaguine, A. A., Richelle, J., and Wodak, S. J. (1999) *Acta Crystallogr. D. Biol. Crystallogr.* **55,** 191–205
24. Dul, J. L., Burrone, O. R., and Argon, Y. (1992) *J. Immunol.* **149,** 1927–1933
25. Davis, D. P., Raffen, R., Dul, J. L., Vogen, S. M., Williamson, E. K., Stevens, F. J., and Argon, Y. (2000) *Immunity* **13,** 433–442
26. Del Pozo Yauner, L., Ortiz, E., Sanchez, R., Sanchez-Lopez, R., Guereca, L., Murphy, C. L., Allen, A., Wall, J. S., Fernandez-Velasco, D. A., Solomon, A., and Becerril, B. (2008) *Proteins* **72,** 684–692
27. Schormann, N., Murrell, J. R., Liepnieks, J. J., and Benson, M. D. (1995) *Proc. Natl. Acad. Sci. U. S. A.* **92,** 9490–9494
28. Palaninathan, S. K., Mohamed Mohaideen, N. N., Snee, W. C., Kelly, J. W., and Sacchettini, J. C. (2008) *J. Mol. Biol.* **382,** 1157–1167